Tiittanen, T.; Karppinen, M.

Magnetic properties and B-site cation ordering in (Sr0.5Ba0.5)2FeSbO6 perovskite

Published in:
Journal of Alloys and Compounds

DOI:
10.1016/j.jallcom.2017.11.366

Published: 15/03/2018

Document Version
Peer reviewed version

Magnetic properties and B-site cation ordering in $(Sr_{0.5}Ba_{0.5})_2FeSbO_6$ perovskite

T. Tiittanen and M. Karppinen*

Department of Chemistry and Materials Science, Aalto University, FI-00076 Espoo, Finland

*maarit.karppinen@aalto.fi

Abstract

We investigate the dependence of magnetic properties on the B-site cation ordering for a series of $(Sr_{0.5}Ba_{0.5})_2FeSbO_6$ double-perovskite samples for which the Fe/Sb long-range ordering ranges from nearly nonexisting to essentially complete. Also the size of crystallographically ordered domains varies among the samples. All the samples are antiferromagnetic at low temperatures independent of the level of ordering, indicating multiple co-existing exchange and/or superexchange interactions. Nevertheless, a clear trend is seen for the Néel temperature and the effective magnetic moment both increasing with increasing degree of order and the size of the ordered domains.

Keywords

double perovskite, degree of order, magnetic properties, antiferromagnetic, exchange and superexchange

1. Introduction

The so-called B-site ordered double-perovskite oxides $A_2B'B''O_6$ accommodate two different metal cation species at the B-cation site in the 1:1 ratio; ordering of the B′ and B″ cations creates two crystallographically distinct sites, effectively seen in the space group which is different for the ordered perovskite from that of the non-ordered perovskite. These $A_2B'B''O_6$ materials have been intensely studied for decades in particular due to their diverse magnetic properties of both scientific and technological interest [1]. In spite of being referred to as B-site ordered perovskites, the ordering between the B′ and B″ cations in $A_2B'B''O_6$ compounds is not always complete, though. The degree of order (DoO) in $A_2B'B''O_6$ compounds is controlled by a number of crystal-chemical and preparative parameters, such as the charge and size difference among the B cations, and the heat-treatment temperature and duration used for the sample synthesis [2,3,4]. The DoO is often expressed using the Bragg-Williams long-range order parameter (S): completely random distribution of the B-site cations gives S = 0, whereas for a fully ordered compound S = 1. Typically, for $A_2B'B''O_6$ compounds with trivalent B′ and pentavalent B″, a range of S values is seen depending on the synthesis conditions.

The degree of B-cation order is an important parameter in controlling the magnetic properties of $A_2B'B''O_6$ double perovskites [1,5,6]. As a notable example, for the room-temperature halfmetallic ferrimagnet Sr_2FeMoO_6 showing tunneling magnetoresistance [7], the magnetic moment and the transition temperature and accordingly the magnetoresistance characteristics have been demonstrated to significantly vary with S [6,8,9,10,11,12,13,14,15,16]. However, despite the apparent impact of the B-cation order on the magnetic properties of $A_2B'B''O_6$ compounds there are very few systematic studies for sample series with a large variance in the S parameter.

Recently, we successfully established appropriate synthesis conditions (temperature and time) to control the DoO in a wide range for the cubic $(Sr_{0.5}Ba_{0.5})_2FeSbO_6$ double perovskite. This compound has trivalent iron (d^5) at the B′ site and pentavalent antimony (d^{10}) at the B″ site, being a member of a larger family of similar $A_2B'B''O_6$ double perovskites, where A = Ca, Sr, Ba, or La or their mixture, B′ = Mn or Fe, and B″ = Nb, Sn, Sb or Te [17,18,19,20,21]. The common nominator for these compounds is that only the B′ site is occupied by a magnetic cation, i.e. either Mn(II) or Fe(III) with the 5/2 spin configuration. If the B′ and B″ cations are fully ordered but their ratio is changed, the magnetic percolation through nearest-neighbor (NN) cations should break up when the content of the magnetic B-site cations is decreased below ca. 30 % [5]. On the other hand, at the B′:B″ ratio of 1:1 as in $(Sr_{0.5}Ba_{0.5})_2FeSbO_6$, estimations show that the NN magnetic percolation (3D superexchange pathways) should break up when the DoO parameter S decreases below ca. 0.70 (i.e. when the fractional occupancy of Fe at its proper site is less than 0.85) [19]. Statistically, for a fully disordered

structure, the number of nearest-neighbors of the same element is three (out of six possible) and the number of next-nearest-neighbor (NNN) cations is six (out of twelve). At S ≈ 0.68 (i.e. the fractional occupancy equals to 0.84) the average numbers are one out of six (zero out of six for fully ordered) for NN and ten out of twelve for NNN [19]. Hence, the percolation apparently breaks up when the number of NN magnetic cations drops just below one. Here, in this work we systematically investigate how the magnetic properties depend on S in $(Sr_{0.5}Ba_{0.5})_2FeSbO_6$.

Previously magnetic properties have been reported for the related antiferromagnetic (AFM) Sr_2FeSbO_6 compound which crystallizes in monoclinic *I*2/*m* space group [17]. The antiferromagnetism arises from the AFM-type stacking of alternating ferromagnetic Fe layers, and the reported Néel temperatures (T_N) have fallen in the narrow range from 35 to 37 K [17,19,22,23,24,25,26]. However, there are no efforts reported so far to systematically clarify how the magnetic properties depend on the DoO in Sr_2FeSbO_6. In the few works that do report the S value, the value has ranged from 0.59 to 0.89. We selected the $(Sr_{0.5}Ba_{0.5})_2FeSbO_6$ composition for our systematic investigation as it is of the ideal cubic *Fm*-3*m* double-perovskite structure; this simplified the structure analysis and the determination of the S parameter [27]. Also, in the cubic non-distorted double perovskite structure, all of the B-site NN interactions should have the same superexchange interaction energy. The same naturally applies to the NNN interactions and therefore there are no preferred interactions among the NN or NNN interactions. This should increase the magnetic frustration [28]. Finally, it should be noted that the Ba_2FeSbO_6 phase is known as well [19], but it is of the hexagonal non-perovskite structure and does not show any long-range magnetic order.

2. Materials and methods

We prepared our $(Sr_{0.5}Ba_{0.5})_2FeSbO_6$ samples through sol-gel synthesis and achieved the precise control of the degree of Fe/Sb order and the size of the ordered domains by carefully selecting the heat-treatment temperature (1050 – 1300 ^oC) and time (0.5 – 100 hours); details of the sample synthesis and structural characterization are found elsewhere [21,27]. In short, the heat treatments were carried out in air for uniaxially-pressed pellets, which were quenched to room temperature after the heat treatment. The samples were confirmed to be of single phase with laboratory XRD (X-ray diffraction; PANalytical X'Pert PRO MPD α-1 powder diffractometer, programmable divergence slits, Johansson monochromator, Cu Kα1 radiation) measurements; the values for S and also for the size of crystallographically ordered domains were determined through Rietveld refinements using the Fullprof software [29].

The magnetic property measurements were performed using a magnetometer (Quantum Design MPMS XL). The sample powders were packed into gelatine capsules, zero-field cooled to 5 K and centered at 1000 Oe field. The zero-field-cooled (ZFC) data were then collected in 2 K steps up to 301 K in 1000 Oe field after which the sample was cooled under an applied field to 5 K while collecting the field-cooled (FC) data.

3. Results and discussion

For the magnetic-properties, we characterized a series of nine single-phase $(Sr_{0.5}Ba_{0.5})_2FeSbO_6$ samples with the DoO parameter S ranging from 0.25 to 0.98; note that also the size of the crystallographically ordered domains varies in the sample series. The samples and their main magnetic characteristics are listed in Table 1. Here it should also be mentioned that for some of the sample compositions (in terms of S and ordered-domain size) we prepared and characterized several parallel samples with highly reproducible results for the magnetic characteristics.

Table 1. Summary of the magnetic properties of our $(Sr_{0.5}Ba_{0.5})_2FeSbO_6$ samples with varying degree of order (S) and size of the crystallographically ordered domain (Domain): Néel temperature (T_N), Weiss temperature (θ), effective magnetic moment (μ_{eff}), deviation temperature from Curie-Weiss law (C-W dev. T) and calculated frustration factor (f).

S	Domain (Å)	T_N (K)	θ (K)	μ_{eff}	C-W dev. T (K)	f
0.25	<100	21.6	-221	5.00	106	10.25
0.32	112	21.6	-208	5.04	74	9.66
0.36	~100	21.6	-239	5.20	74	11.06
0.62	312	27.6	-220	5.25	70	7.96
0.69	98	21.6	-225	5.35	66	10.42
0.71	256	23.6	-219	5.26		11.43
0.91	527	33.6	-197	5.13	81	5.85
0.96	860	31.6	-191			6.04
0.98	743	36.6	-236	5.45		7.28

All the samples independent of the degree of Fe/Sb order show the paramagnetic to antiferromagnetic transition at low temperatures; in Figure 1 we show the magnetic susceptibility versus temperature curves for selected samples. Since our sample series constitutes of samples with a large variation in S such that the number of magnetic (Fe(III)) nearest neighbors varies from essentially zero to nearly three, it thus seems that not the NN but the NNN superexchange interactions must have a major contribution to the antiferromagnetism in $(Sr_{0.5}Ba_{0.5})_2FeSbO_6$. Another explanation for the presence of long-range magnetic order in all of our samples (even though the NN magnetic

percolation is expected to break up when S at ca. 0.70; c.f. the discussion in Introduction) could be the involvement of two or more interactions that in cooperation bring rise to the long-range AFM order, as in Sr_2CrRuO_6, not to rule out the ferri- or ferromagnetic interactions [28,30].

The Néel temperature, taken at the maximum susceptibility in the para- to antiferromagnetic transition region, falls between 21.6 and 36.6 K for the nine samples measured. For comparison, the highest T_N value reported for Sr_2FeSbO_6 is ca. 37 K [23], which is notably close to our highest T_N value of 36.6 K. Also, we synthesized and characterized a reference Sr_2FeSbO_6 sample through a similar synthesis route as used for the $(Sr_{0.5}Ba_{0.5})_2FeSbO_6$ samples: for our Sr_2FeSbO_6 sample S was determined at 0.90 and T_N at ca. 37 K.

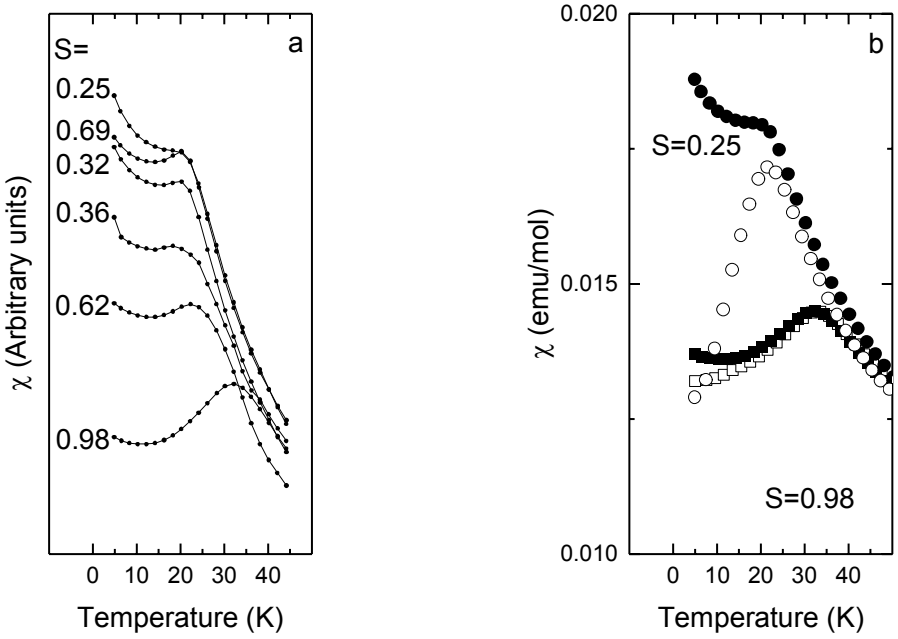

Figure 1. Magnetic susceptibility χ versus temperature curves measured (a) in FC mode for six representative samples with different S values, and (b) in both FC (black markers) and ZFC (white markers) modes for the two end members in the sample series.

From Figure 1(a), it is seen that T_N increases with increasing S. To clarify this trend in more detail, we plot in Figure 2(a) the T_N value against the DoO parameter S for all the nine samples investigated. It is seen that T_N indeed increases with S in general, but not in a linear manner. The nonlinearity could be explained by the fact that for our samples also the size of the crystallographically ordered domains varies. In particular the sample with S = 0.69 is a clear outlier in the T_N versus S plot; this is a sample which has a prominently small ordered-domain size (Table 1). It thus seems that T_N could depend on the size of the ordered domains as well. From Figure 2(b)

where we plot T_N against the domain size it can be seen that the dependency is nearly linear. This linearity could suggest that T_N in $(Sr_{0.5}Ba_{0.5})_2FeSbO_6$ depends even more strongly on the ordered-domain size than the DoO parameter S. Similar magnetic-property dependencies on DoO and ordered-domain size have been seen for some multiferroic systems as well, but with an opposite effect on T_N [31,32]. It should be mentioned that we made an effort to study the finite-size effect on T_N. However, the scaling laws applied elsewhere [33] did not produce reasonable results for our ordered-domain size versus T_N relation. This is presumably due to the differences in the systems, i.e. magnetic particles versus ordered magnetic domains within particles.

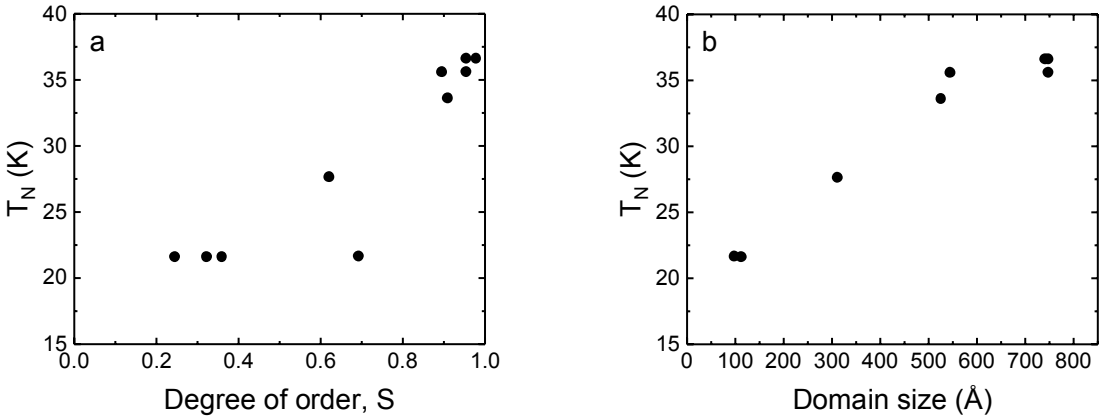

Figure 2. Néel temperature T_N as a function of (a) the DoO parameter S, and (b) and the size of crystallographically ordered domains; the estimated error bars for S and domain size [27] are within size of the datum-point markers.

We fitted the magnetization data in the paramagnetic region to the Curie-Weiss (C-W) law for all the samples it was possible. For example, for the nearly randomly ordered S = 0.25 sample where also the size of the crystallographically ordered domains is small (Table 1), the C-W law applies well down to ca. 106 K; with increasing S the deviation temperature from the C-W law somewhat decreases, being at the lowest ca. 66 K for the S = 0.69 sample (Table 1). This indicates that the spin freezing starts at higher temperatures for the poorly ordered samples than in the highly ordered samples, and that the spins close to the domain boundaries remain dynamic down to low temperatures.

The effective magnetic moment (μ_{eff}) was calculated from the slope of the linear part of the Curie-Weiss plot using equation

$$\mu_{eff} = \sqrt{\frac{3k}{N\mu_B^2}}\sqrt{T\chi}, \qquad (1)$$

where k is Boltzmann constant, N is Avogadro number, μ_B is Bohr magneton, T is temperature in Kelvins and χ is molar magnetic susceptibility ($T\chi$ = 1/slope). The resultant μ_{eff} values are listed in

Table 1. A weak trend of increasing effective magnetic moment with increasing DoO can be revealed, from ca. 5.0 μ_B for the S = 0.25 sample up to ca. 5.45 μ_B for the S = 0.98 sample. This could be attributed to the decreasing concentration of antiphase boundaries [12,13,34]. In overall, the μ_{eff} values obtained for the samples are quite close to the theoretical μ_{eff} value of 5.92 calculated assuming high-spin Fe(III).

The interaction energy (J) is thought to be directly related to the Néel temperature, i.e. $J = kT_N$. At T_N the magnetic domains span over the crystallographically ordered domains. Since the Weiss temperatures are clearly negative in our $(Sr_{0.5}Ba_{0.5})_2FeSbO_6$ samples (Table 1), all the exchange interaction energies are negative. A prominent feature of some of the magnetization curves for the samples (see Figure 1(b)) is the large irreversibility between the ZFC and FC curves, especially in samples with a low DoO and a small ordered-domain size. This may be attributed to the lack of order and subsequent presence of antiphase boundaries and domain wall pinning, as seen in diluted 2D and 3D antiferromagnetic systems [5,35,36].

In Figure 1, the low-temperature tail seen in the FC susceptibility curves below T_N in particular for the poorly ordered samples can be explained by the concentration of crystallographic domains and their boundaries. The number of ordered domains within crystallites and therefore the concentration of domain boundaries is usually larger for the less ordered samples than for the highly ordered, large-domain samples. Magnetic domains are naturally pinned by the crystallographic domain walls and separated by either a non-ordered region or antiphase boundaries [5,19,35,36]. Hence there remains a certain number on unpaired/uncompensated spins at domain boundaries, contributing to the rising tail. This is very similar to the behavior seen in Sr_2FeMoO_6 in which there exists a two atom thick layer of Fe cations at the antiphase boundaries; the spins of the Fe cations at the antiphase boundaries act independently in contrast to the bulk of the neighboring domains [37].

We calculated the magnetization (M) for the unpaired paramagnetic spins as [38]

$$M = N\mu_B \tanh\left(\frac{\theta\beta}{2}\right),$$

where

$$\theta = 2\mu_B H \text{ and } \beta = \frac{1}{kT}$$

and H is the applied magnetic field. In Figure 3 we show the calculated paramagnetic contribution fitted and drawn into the FC curve. Also, the FC curve with subtracted paramagnetism is drawn, and it shows a plateau below T_N, which is typical for antiferromagnetic materials. When the sample is cooled in an absence of field, individual magnetic domains freeze with random orientations. The non-zero AFM contribution rises from the AFM domains aligned with the field and from the domain

boundary/surface paramagnetism. When the sample is heated in a magnetic field, the AFM domains start to align with the field, reaching the maximum alignment at T_N, but being yet slightly misaligned (canted AFM-like behavior); this is seen as the lower value of susceptibility at T_N. When the sample is field cooled and the spin freezing occurs, all AFM domains are aligned and the susceptibility at T_N is slightly higher than what it is for the ZFC case [8]. With higher measuring fields, the difference between the ZFC and FC curves should disappear, but at the same time one would lose the detailed magnetic information. Therefore, the contribution from unpaired spin paramagnetism decreases (with increasing T_N) as the DoO and/or domain size increase.

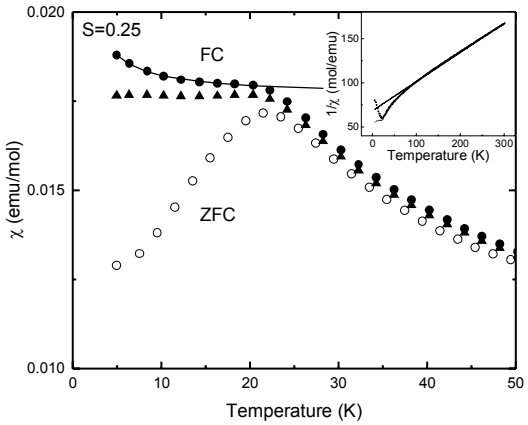

Figure 3. Illustration of the typical irreversibility seen in the magnetic susceptibility for a poorly ordered (S = 0.25) sample with small crystallographic domains, and its fitting for the unpaired spin paramagnetism (black line): ZFC (white circles), FC (black circles), and the FC susceptibility after subtraction of the paramagnetism (black triangles). The unpaired spin paramagnetism curve is offset such that it is in alignment with the FC curve. Reciprocal magnetic susceptibility is shown in the inset.

Finally, we like to note that some magnetic frustration is indeed present in our $(Sr_{0.5}Ba_{0.5})_2FeSbO_6$ samples, as the frustration factors (f) calculated from the Weiss temperatures (θ) [27] are clearly higher than 3, or even above the borderline value of 10 of the significantly frustrated systems. From Table 1, where we list the calculated frustration factors, a trend of increasing f with decreasing DoO can be seen.

Conclusions

With a series of single-phase samples of the $(Sr_{0.5}Ba_{0.5})_2FeSbO_6$ double perovskite in which both the degree of order among the B-site cations and the size of the crystallographically ordered domains vary in wide ranges, we have been able to gain a comprehensive picture of the interplay between the

cation ordering and magnetic properties. The characteristic features of this selected double-perovskite model system are the cubic crystal structure and the fact that the B-cation site is occupied by magnetic (d^5 Fe(III)) and non-magnetic (d^{10} Sb(V)) cations.

We found that independent of the degree of order, all our samples were antiferromagnetic, even those for which the degree of order was below the threshold limit of around S = 0.70 expected for the realization of magnetic percolation. This interesting observation was discussed by tentatively proposing either NNN superexchange interaction being the dominant at defining the magnetic ordering or that multiple co-operative interactions are responsible for the long-range AFM ordering.

With enhancing B-site cation ordering and/or increasing ordered-domain size, a clear trend of increasing Néel temperature by ca. 15 K could be revealed. This seemed to be accompanied with a decrease in the magnetic frustration. For the poorly ordered samples a tail in magnetic susceptibility below T_N was seen, which decreased with the progress in ordering/domain growth. The tail was tentatively attributed to the increased number of unpaired/uncompensated AFM spins and/or crystallographic domain boundaries in the poorly ordered samples.

References

[1] S. Vasala, M. Karppinen, Prog. Solid State Chem. 43 (2015) 1–36
[2] P. M. Woodward, R. D. Hoffmann, A. W. Sleight. J. Mater. Res. 9 (1994) 2118–2127
[3] G. King, P. M. Woodward, J. Mater. Chem. 20 (2010) 5785–5796
[4] T. Shimada, J. Nakamura, T. Motohashi, H. Yamauchi, M. Karppinen, Chem. Mater. 15 (2003) 4494–4497
[5] T. C. Gibb, R. J. Whitehead, J. Mater. Chem. 3 (1993) 591–596
[6] C. Meneghini, S. Ray, F. Liscio, F. Bardelli,S. Mobilio, D. D. Sarma, Phys. Rev. Lett. 103 (2009) 046403-1–4
[7] K. L. Kobayashi, T. Kimura, H. Sawada, K. Terakura, Y. Tokura, Nature 395 (1998) 677–680
[8] Y. H. Huang, J. Lindén, H. Yamauchi, H. Karppinen, Chem. Mater. 16 (2004) 4337–4342
[9] L. Ortega-San Martin, J. P. Chapman, L. Lezama, J. J. S. Garitaonandia, J. S. Marcos, J. Rodríguez-Fernández, M. I. Arriortua, T. Rojo, J. Mater. Chem. 16 (2006) 66–76
[10] Y. H. Huang, M. Karppinen, H. Yamauchi, J. B. Goodenough, Phys. Rev. B 73 (2006) 104408-1–5
[11] Y. Yasukawa, J. Lindén, T.S. Chan, R. S. Liu, H. Yamauchi, M. Karppinen, J. Solid State Chem. 177 (2004) 2655–2662
[12] Ll. Balcells, J. Navarro, M. Bibes, A. Roig, B. Martínez, J. Fontcuberta, Appl. Phys. Lett. 78 (2001) 781–783
[13] A. S. Ogale, S. B. Ogale, R. Ramesh, T. Venkatesan, Appl. Phys. Lett. 75 (1999) 537–539
[14] M. García-Hernández, J. L. Martínez, M. J. Martínez-Lope, M. T. Casais, J. A. Alonso, Phys. Rev. Lett. 86 (2001) 2443–2446
[15] D. D. Sarma, S. Ray, K. Tanaka, M. Kobayashi, A. Fujimori, P. Sanyal, H. R. Krishnamurthy, C. Dasgupta, Phys. Rev. Lett. 98 (2007) 157205-1–4
[16] X.H. Lia, Y. P. Suna, W. J. Lua, R. Anga, S.B. Zhanga, X.B. Zhua, W.H. Songa, J.M. Dai, Solid State Commun. 145 (2008) 98–102
[17] A. Faik, J. M. Igartua, E. Iturbe-Zabalo, G. J. Cuello, J. Mol. Struct. 963 (2010) 145–152
[18] S.-O. Lee, T. Y. Cho, S.-H. Byeon, Bull. Korean Chem. Soc. 18 (1997) 91–97
[19] P. D. Battle, T. C. Gibb, A. J. Herod, J. P. Hodges, J. Mater. Chem. 5 (1995) 75–78
[20] K. Tezuka, K. Henmi, Y. Hinatsu, N. M. Masaki, J. Solid State Chem. 154 (2000) 591–597
[21] T. Tiittanen, M. Karppinen, J. Solid State Chem. 246 (2017) 245–251
[22] G. Blasse, J. Inorg. Nucl. Chem. 27 (1965) 993–1003.
[23] E. J. Cussen, J. F. Vente, P. D. Battle, T. C. Gibb, J. Mater. Chem. 7 (1997) 459–463
[24] N. Kashima, K. Inoue, T. Wada, Y. Yamaguchi, Appl. Phys. A 74 (2002) S805–S807

[25] M. Retuerto, F. Jiménez-Villacorta, M. J. Martínez-Lope, Y. Huttel, E. Roman, M. T. Fernández-Díaz, J. A. Alonso, Phys. Chem. Chem. Phys. 12 (2010) 13616–13625
[26] M. Maryško, V. V. Laguta, I. P. Raevski, R. O. Kuzian, N. M. Olekhnovich, A. V. Pushkarev, Y. V. Radyush, S. I. Raevskaya, V. V. Titov, S. P. Kubrin, AIP ADVANCES 7 (2017) 056409 -1–6
[27] T. Tiittanen, M. Karppinen, J. Solid State Chem. 258 (2018) 11–14
[28] J.-W. G. Bos, J. P. Attfield, Phys. Rev. B 70 (2004) 174434-1–8
[29] J. Rodriguez-Carvajal, Physica B 192 (1993) 55–69
[30] J. A. Rodgers, A. J. Williams, M. J. Martinez-Lope, J. A. Alonso, J. P. Attfield, Chem. Mater. 20 (2008) 4797–4799
[31] C. Upadhyay, P. K. Harijan, A. Senyshyn, R. Ranganathan, D. Pandey, Appl. Phys. Lett. 106 (2015) 093103-1–5
[32] V. V. Laguta, M. D. Glinchuk, M. Maryško, R. O. Kuzian, S. A. Prosandeev, S. I. Raevskaya, V. G. Smotrakov, V. V. Eremkin, I. P. Raevski, Phys. Rev. B 87 (2013) 064403-1–8
[33] X. Batlle, A. Labarta, J. Phys. D: Appl. Phys. 35 (2002) R15–R42
[34] J. Navarro, L. l. Balcells, F. Sandiumenge, M. Bibes, A. Roig, B. Martínez, J. Fontcuberta, J. Phys.: Condens. Matter 13 (2001) 8481–8488
[35] T. C. Gibb, J. Mater. Chem. 9 (1999) 2851–2858
[36] T. C. Gibb, J. Mater. Chem. 11 (2001) 456–463
[37] J. Lindén, M. Karppinen, T. Shimada, Y. Yasukawa, H. Yamauchi, Phys. Rev. B 68 (2003) 174415-1–5
[38] S. Sahling, G. Remenyi, C. Paulsen,P. Monceau, V. Saligrama, C. Marin, J. E. Lorenzo, Nature Phys. 11(3) (2015) 255–260